

**UNIVERSIDADE DE SÃO PAULO**

**INSTITUTO DE FÍSICA  
CAIXA POSTAL 66318  
05389-970 SÃO PAULO - SP  
BRASIL**

# **PUBLICAÇÕES**

*lymo*: 2178828  
**IFUSP/P-1176**

**THE SU (3) LIPKIN MODEL. (II):  
THE THERMAL CHAOTIC CLASSICAL DYNAMICS**

**M.O. Terra**

Instituto de Física, Universidade de São Paulo

**A.H. Blin, B. Hiller, C. Providência and J. da Providência**  
Centro de Física Teórica (INIC), Universidade de Coimbra,  
P-3000 Coimbra, Portugal

**M.C. Nemes**

Departamento de Física, Instituto de Ciências Exatas,  
Universidade Federal de Minas Gerais,  
C.P. 702,31270 Belo Horizonte, MG, Brazil

Setembro/1995

# The SU(3) Lipkin model. (II): The thermal chaotic classical dynamics

## I. INTRODUCTION

M.O.Terra<sup>1</sup>, A.H.Blin<sup>2</sup>, B.Hiller<sup>2</sup>, M.C.Nemes<sup>3</sup>,  
C.Providência<sup>2</sup> and J. da Providência<sup>2</sup>

<sup>1</sup> *Instituto de Física, Departamento de Física-Matemática, Universidade de São Paulo, C.P. 66318, São Paulo, SP, Brazil.*

<sup>2</sup> *Centro de Física Teórica (INIC), Universidade de Coimbra, P-3000 Coimbra, Portugal.*

<sup>3</sup> *Departamento de Física, Instituto de Ciências Exatas, Universidade Federal de Minas Gerais, C.P. 702, 31270 Belo Horizonte, MG, Brazil.*

### Abstract

In the present work we study temperature effects on the classical dynamics of the SU(3) Lipkin model. We show that the inclusion of thermal effects gives rise to a new degree of freedom, absent in the zero temperature limit. The existence conditions of stationary points and bifurcations are studied as a function of temperature. The dynamical structure of the classical equations is very rich: contrasting results recently found for the Maser model, we show that temperature effects give rise to new nonlinear contributions.

The underlying classical phase space structure of quantum models which exhibit chaotic behavior is of fundamental importance in the context of semiclassical quantum mechanics: Such classical structure is usually defined by the variational parameters which characterize a mean field approximation over a family of appropriate coherent states. This approach has recently been used to characterize the structure of eigenfunctions in terms of classical trajectories in the SU(3) Lipkin model [1]. In this particular case the classical limit of the model was obtained as the limit when the number of particles  $N$  goes to infinity and by using the appropriate coherent states, parameterized by two complex variables [2]. The classical two degrees of freedom equations of motion obtained are shown to exhibit fourteen stationary points whose stability as a function of the coupling strength were found analytically.

In the present contribution we intend to study how the phase space structure and fixed points analysis is altered if one introduces temperature in the dynamics. In other words we use a thermal mean field approach [3] in order to introduce the temperature in the problem. The first interesting consequence of introducing temperature in the dynamical equations is the appearance of a third degree of freedom. Also important are the restrictions imposed on the phase space due to the thermal dynamics. The temperature effects on the dynamics of the model is far more intricated than in the recently case of the Maser model [4] where only a phase space scaling effect is found.

In the general thermal Lipkin SU(3) model the phase space structure is defined by three complex variational parameters. We were not able to find the corresponding three pairs of canonically conjugate variables. However, in the strong coupling regime (SCR), i.e., for temperatures not too high as compared to the coupling strength we were able to show that the problem reduces to only two pairs of canonically conjugate variables and still maintain most of the new thermal effects under discussion. In this case we give detailed account of the stability and bifurcation of equilibria of the (also) fourteen points as a function of coupling strength and temperature. We observe that in the SCR raising the temperature corresponds effectively to weakening the coupling strength. Although the new terms in the Hamiltonian show a rather non trivial behavior with temperature (e.g. it does not consist of pure scaling effect, but brings novel nonlinearities), in the SCR this is not seen in the Poincaré sections.

In section II we briefly present the model and in section III we construct the thermal dynamics of the problem and its small amplitude limit. The large amplitude motion in the strong coupling regime is studied in section IV and in section V its fixed points and bifurcations are analysed. Poincaré sections of the thermal dynamics are presented in this regime in the section VI. Concluding remarks are in the last section.

## II. THE 3-LEVEL LIPKIN MODEL [1, 2, 5, 6]

The 3-level Lipkin-Meshkov-Glick model is an exactly soluble schematic shell

model. In this model,  $N$  interacting fermions are distributed between three  $N$ -fold degenerate levels with energies  $\epsilon_0$ ,  $\epsilon_1$  and  $\epsilon_2$ ; each single particle state is labeled by two numbers,  $\alpha = 0, 1, 2$  denoting the orbital and  $p = 1, 2, \dots, N$  referring to the degenerate state on a given level. In our calculations, we have chosen  $\epsilon_2 = -\epsilon_0 = \epsilon$  and  $\epsilon_1 = 0$ . The Hamiltonian is given by

$$H = \epsilon(G_{22} - G_{00}) + \frac{V}{2} (G_{12}^2 + G_{21}^2 + G_{20}^2 + G_{02}^2 + G_{10}^2 + G_{01}^2), \quad (1)$$

where  $V$  is the interaction strength, the generators  $G_{ij}$  satisfy the commutation rules

$$[G_{ij}, G_{kl}] = \delta_{jk}G_{il} - \delta_{il}G_{kj} \quad (2)$$

and obey the relation  $G_{00} + G_{11} + G_{22} = N$ . In terms of the creation (annihilation) operators  $a_{pi}^\dagger$  ( $a_{pi}$ ) which create (annihilate) a particle in the level  $i$  state  $p$ , the operators  $G_{ij}$  are written as

$$G_{ij} = \sum_{p=1}^N a_{pi}^\dagger a_{pj}, \quad G_{ij}^\dagger = G_{ji}, \quad i, j = 0, 1, 2. \quad (3)$$

In the present work all the energies are given in units of  $N\epsilon$ . The scaled coupling constant is defined as  $\chi = \frac{N(V-1)}{\epsilon}$ , as usual.

## III. FINITE TEMPERATURE DYNAMICS AND ITS SMALL AMPLITUDE LIMIT

The procedure we follow in this section to derive the finite temperature dynamics of the system is well established and we shall therefore limit ourselves to its application in the present case [3].

We start by introducing the thermal classical Lagrangian of the system ( $\hbar = 1$ ),

$$L = i \text{Tr}(DU\dot{U}^\dagger) - \text{Tr}(DUHU^\dagger), \quad (4)$$

where  $U$  has the form

$$U = U_3 U_2 U_1 = e^{is_3(t)} e^{is_2(t)} e^{is_1(t)}, \quad (5)$$

with

$$s_1(t) = z_1(t)G_{10} + z_1^*(t)G_{01}, \quad (6)$$

$$s_2(t) = z_2(t)G_{20} + z_2^*(t)G_{02}, \quad (7)$$

$$s_3(t) = z_3(t)G_{21} + z_3^*(t)G_{12}, \quad (8)$$

and  $D$  is the diagonal form of density  $D_0$  given by

$$D = UD_0U^\dagger = \frac{1}{Z} e^{\beta_1(G_{11}-G_{00})} e^{\beta_2(G_{22}-G_{00})}, \quad (9)$$

where

$$Z = z^N = \text{Tr}(e^{\beta_1(G_{11}-G_{00})} e^{\beta_2(G_{22}-G_{00})}), \quad (10)$$

$$z = e^{\beta_1} + e^{\beta_2} + e^{-(\beta_1+\beta_2)}, \quad (11)$$

$$D_0 = K \exp(-\beta h_{MF}), \quad (12)$$

$$h_{MF} = \alpha_1(G_{11} - G_{00}) + \alpha_2 G_{01} + \alpha_2^* G_{10} + \alpha_3(G_{22} - G_{00}) + \alpha_4 G_{02} + \alpha_4^* G_{20} + \alpha_5(G_{11} - G_{22}) + \alpha_6 G_{12} + \alpha_6^* G_{21}, \quad (13)$$

and  $K$  is a normalization factor.

The definition of classical variables comes from the first term on the r.h.s. of eq.

(4). We get

$$\begin{aligned} \text{Tr}(DU\dot{U}^\dagger) = & \frac{\dot{z}_3 z_3^* - z_3 \dot{z}_3^*}{2z_3 z_3^*} S_3^2 \tilde{T}_3 + \frac{\dot{z}_2 z_2^* - z_2 \dot{z}_2^*}{2z_2 z_2^*} S_2^2 (\tilde{T}_2 - S_3^2 \tilde{T}_3) + \\ & + \frac{\dot{z}_1 z_1^* - z_1 \dot{z}_1^*}{2z_1 z_1^*} S_1^2 \{ \tilde{T}_1 + S_3^2 \tilde{T}_3 - S_2^2 (\tilde{T}_2 - S_3^2 \tilde{T}_3) + \\ & + i \frac{(z_1 z_2^* z_3 - z_1^* z_2 z_3^*)}{\sqrt{z_1 z_1^*} \sqrt{z_2 z_2^*} \sqrt{z_3 z_3^*}} \frac{C_1 S_2 S_3 C_3}{S_1} \tilde{T}_3 \} + \\ & + i \frac{(z_1 z_1^* + z_1 \dot{z}_1^*)}{2z_1 z_1^*} (z_1 z_2^* z_3 + z_1^* z_2 z_3^*) \frac{S_2 S_3 C_3}{\sqrt{z_2 z_2^*} \sqrt{z_3 z_3^*}} \tilde{T}_3 \end{aligned} \quad (14)$$

with

$$S_j = \sin \sqrt{z_j z_j^*}, \quad C_j = \cos \sqrt{z_j z_j^*}, \quad j = 1, 2, 3; \quad (15)$$

$$\tilde{T}_1 = N T_1 = \text{Tr}(D(G_{00} - G_{11})) = N \frac{e^{-(\beta_1+\beta_2)} - e^{\beta_1}}{z}, \quad (16)$$

$$\tilde{T}_2 = N T_2 = \text{Tr}(D(G_{00} - G_{22})) = N \frac{e^{-(\beta_1+\beta_2)} - e^{\beta_2}}{z}, \quad (17)$$

and

$$\tilde{T}_3 = \tilde{T}_2 - \tilde{T}_1 = \text{Tr}(D(G_{11} - G_{22})). \quad (18)$$

In principle for an arbitrary initial condition ( $\beta_1$  and  $\beta_2$ ) we have three pairs of noncanonical variables. We may choose  $\beta_1$  and  $\beta_2$  to correspond to a thermodynamical equilibrium state. The second term on the r.h.s. of eq. (4) is the classical counterpart of the quantum hamiltonian of the system defined in section II. In terms of the variables  $z_1, z_2$  and  $z_3$  it is given by

$$\begin{aligned}
\frac{\mathcal{H}(z_i, z_i^*)}{N} = & (-1 + 2S_2^2)(T_2 - S_3^2 T_3) + i(z_1 z_2^* z_3 - z_1^* z_2 z_3^*) \frac{S_1 C_1 S_2 S_3 C_3}{R_1 R_2 R_3} T_3 + \\
& + S_1^2 \{T_1 + S_3^2 T_3 - S_2^2 (T_2 - S_3^2 T_3)\} + \frac{\chi}{2} \left\{ -(z_1^2 + z_1^{*2}) \left( \frac{S_1 C_1}{R_1} \right)^2 \right. \\
& \cdot \left. \{T_1 + S_3^2 T_3 - S_2^2 (T_2 - S_3^2 T_3)\}^2 + [(z_2 z_3^*)^2 + (z_2^* z_3)^2] C_1^4 + \right. \\
& + \left. \left[ \left( \frac{z_1 z_2^* z_3}{z_1^*} \right)^2 + \left( \frac{z_1^* z_2 z_3^*}{z_1} \right)^2 \right] S_1^4 + 2 \left( \frac{z_1}{z_1^*} + \frac{z_1^*}{z_1} \right) R_2^2 R_3^2 C_1^2 S_1^2 \right\} \cdot \\
& \cdot \left( \frac{S_2 S_3 C_3}{R_2 R_3} \right)^2 T_3^2 + \left\{ (z_1 z_2 z_3^* - z_1^* z_2^* z_3) C_1^2 + \left( \frac{z_1^2 z_2^* z_3}{z_1^*} - \frac{z_1^{*2} z_2 z_3^*}{z_1} \right) S_1^2 \right\} \cdot \\
& \cdot 2i \frac{S_1 C_1 S_2 S_3 C_3}{R_1 R_2 R_3} T_3 [T_1 + S_3^2 T_3 - S_2^2 (T_2 - S_3^2 T_3)] - (z_2^2 + z_2^{*2}) \cdot \\
& \cdot \left( \frac{C_1 S_2 C_2}{R_2} \right)^2 (T_2 - S_3^2 T_3)^2 + [(z_1 z_3)^2 + (z_1^* z_3^*)^2] \left( \frac{S_1 C_2 S_3 C_3}{R_1 R_3} \right)^2 T_3^2 + \\
& - 2i (z_1 z_2 z_3 - z_1^* z_2^* z_3^*) \frac{S_1 C_1 S_2 C_2^2 S_3 C_3}{R_1 R_2 R_3} T_3 (T_2 - S_3^2 T_3) - (z_3^2 + z_3^{*2}) \cdot \\
& \cdot \left( \frac{C_1 C_2 S_3 C_3}{R_3} \right)^2 T_3^2 + [(z_1^* z_2)^2 + (z_1 z_2^*)^2] \left( \frac{S_1 S_2 C_2}{R_1 R_2} \right)^2 [T_2 - S_3^2 T_3]^2 + \\
& - 2i (z_1^* z_2 z_3 - z_1 z_2^* z_3^*) \frac{S_1 C_1 S_2 C_2^2 S_3 C_3}{R_1 R_2 R_3} T_3 (T_2 - S_3^2 T_3) \}. \quad (19)
\end{aligned}$$

One interesting point to remark now is that the effects of the temperature, in contrast to the results encountered for the Maser model [4], are far richer. It is not a simple phase space scaling effect, as found in ref.[4]. Also, in principle one could now proceed to investigate the full thermal dynamical behavior of the system. This

calculation although feasible is highly non trivial and cumbersome. However the most interesting new feature brought by the temperature on the dynamics of the system is the "awakening" of a new degree of freedom,  $z_3$ , absent for zero temperature. Unfortunately we were not able to cast eq. (14) in the form of canonical variables for all three degrees of freedom. However we can study this new effect by means of considering small amplitude motion.

The quantities  $T_1, T_2$  and  $T_3$  are very important in the study of the dynamics. They have been obtained in ref. [7] for attractive interaction ( $\chi < 0$ ) and are displayed in Fig. 1 as function of inverse temperature for  $\chi = -6.0$ .

#### A. Small amplitude motion for the full system

The small amplitude fluctuations around equilibrium are described by the second order Lagrangian

$$\mathcal{L}^{(2)} = \sum_{i=1}^3 \frac{i}{2} (\dot{\gamma}_i \gamma_i^* - \gamma_i \dot{\gamma}_i^*) - \mathcal{H}^{(2)}(\gamma_i, \gamma_i^*), \quad (20)$$

with

$$\mathcal{H}^{(2)}(\gamma_i, \gamma_i^*) = \frac{1}{2} \begin{pmatrix} \gamma_1^* & \gamma_2^* & \gamma_3^* & \gamma_1 & \gamma_2 & \gamma_3 \end{pmatrix} \begin{pmatrix} A & B \\ B & A \end{pmatrix} \begin{pmatrix} \gamma_1 \\ \gamma_2 \\ \gamma_3 \\ \gamma_1^* \\ \gamma_2^* \\ \gamma_3^* \end{pmatrix}, \quad (21)$$

where the variables  $\gamma_i, \gamma_i^*, i = 1, 2, 3$  are canonical variables related to the small deviations,  $\delta z_i, \delta z_i^*$ , from the equilibrium solution and  $A, B$  are  $3 \times 3$  matrices which will be defined according to the different phases. These three phases were extensively studied in ref.[7], their validity ranges illustrated in Fig. 1. From now on we discuss the small amplitude motion in the three possible regimes found there. The RPA frequencies are given by the equation

$$\Omega_i^2 u = (A + B) \cdot (A - B) u, \quad i = 1, 2, 3. \quad (22)$$

### 1. The weak coupling regime (WCR)

The state of statistical equilibrium (absolute minimum) is defined by

$$z_1 = z_2 = z_3 = 0, \quad \beta_1 = 0, \quad \beta_2 = -\beta \quad (23)$$

and has the following energy and free energy

$$\frac{E_0}{N} = -T_2, \quad \frac{F_0}{N} = -\frac{1}{\beta} (\ln[1 + 2 \cosh(\beta)]). \quad (24)$$

In this regime we introduce the canonical variables

$$\gamma_1 = \delta z_1 \sqrt{T_1}, \quad \gamma_2 = \delta z_2 \sqrt{T_2}, \quad \gamma_3 = \delta z_3 \sqrt{T_3} \quad (25)$$

and the RPA matrices  $A, B$  are given by

$$A = \begin{pmatrix} 1 & 0 & 0 \\ 0 & 2 & 0 \\ 0 & 0 & 1 \end{pmatrix} \quad B = \begin{pmatrix} -\chi T_1 & 0 & 0 \\ 0 & -\chi T_2 & 0 \\ 0 & 0 & -\chi T_3 \end{pmatrix}. \quad (26)$$

We obtain the following RPA frequencies:

$$\Omega_1 = \sqrt{1 - \chi^2 T_1^2}, \quad \Omega_2 = \sqrt{4 - \chi^2 T_2^2}, \quad \Omega_3 = \sqrt{1 - \chi^2 T_3^2}. \quad (27)$$

The transition to the intermediate coupling regime occurs for  $\chi^2 T_1^2 = 1$ , therefore the weak coupling region is defined by

$$|\chi| \leq \frac{1}{T_1}. \quad (28)$$

### 2. The intermediate coupling regime (ICR)

The state of statistical equilibrium (two symmetric minima) is defined by

$$z_1 = -z_1^* = \pm ia, \quad \cos(2a) = \frac{-1}{\chi T_1}, \quad (29)$$

$$z_2 = z_3 = 0, \quad (30)$$

$$\ln \left( \frac{P_2^2}{P_0 P_1} \right) = -3\beta, \quad \ln \left( \frac{P_2 P_1}{P_0^2} \right) = -\frac{3\beta}{2} (T_1 \chi - 1), \quad (31)$$

where  $P_j = \text{Tr}(DG_{jj})$ ,  $j = 0, 1, 2$ . Its energy per particle is

$$\frac{E_0}{N} = -T_2 + T_1 \sin^2(a) + \frac{T_1 \chi \sin^2(2a)}{4}. \quad (32)$$

We introduce the canonical variables

$$\gamma_1 = \delta z_1 \sqrt{T_1 \sin(2a)/2a}, \quad \gamma_2 = \delta z_2 \sqrt{T_2}, \quad \gamma_3 = \delta z_3 \sqrt{T_3}, \quad (33)$$

and obtain for the RPA matrices in terms of  $a$ :

$$A_{ij} = B_{ij} = 0, \quad i \neq j \quad (34)$$

$$A_{11} = \frac{\csc(2a)}{2a} \left( a \sin(2a) + 2a^2 \cos(2a) + \frac{\chi}{2} T_1 (a \sin(4a) - 2 \sin^2(2a) + 4a^2 \cos(4a)) \right),$$

$$A_{22} = 2 - \sin^2(a) - \frac{\chi}{2} T_1 \sin^2(2a), \quad A_{33} = 1 + \sin^2(a) + \frac{\chi}{2} T_1 \sin^2(2a),$$

$$B_{11} = \frac{\csc(2a)}{2a} \left( a \sin(2a) - 2a^2 \cos(2a) + \frac{\chi}{2} T_1 (a \sin(4a) - 2 \sin^2(2a) - 4a^2 \cos(4a)) \right),$$

$$B_{22} = -T_2 \chi, \quad B_{33} = -T_3 \chi.$$

The RPA frequencies are :

$$\Omega_1 = \sqrt{2[(\chi T_1)^2 - 1]}, \quad (35)$$

$$\Omega_2 = \frac{1}{2} \sqrt{[(3 - \chi T_1)^2 - (2\chi T_2)^2]}, \quad (36)$$

$$\Omega_3 = \frac{1}{2} \sqrt{[(3 + \chi T_1)^2 - (2\chi T_3)^2]}. \quad (37)$$

The transition to the strong coupling regime occurs for  $\chi T_1 \leq -3$ .

### 3. Strong coupling regime (SCR)

In this regime the state of statistical equilibrium (four minima) occurs for  $\beta_1 = \beta_2$ ,  $T_3 = 0$ ,  $T_1 = T_2$  and therefore the behavior of the system is independent of the value

of the variables  $z_3, z_3^*$ . The variables  $\gamma_i, \gamma_i^*$  are pure imaginary,  $\gamma_1 = -\gamma_1^* = \pm ia$ ,  $\gamma_2 = -\gamma_2^* = \pm ib$ , where  $a^2 = T_1/3$  and  $b^2 = (3 + T_1 \chi)/(3\chi)$  and the energy has the value

$$E_0 = -T_1 + a^2 + 2b^2 + \chi \left( (a^2 + b^2)(T_1 - a^2 - b^2) + a^2 b^2 \right). \quad (38)$$

The RPA matrices in terms of  $a$  and  $b$  have the form

$$A = \begin{pmatrix} 1 - \chi(3a^2 + b^2) & 0 \\ 0 & 2 - \chi(a^2 + 3b^2) \end{pmatrix}, \quad B = \begin{pmatrix} \chi(3a^2 - T_1) & 2ab\chi \\ 2ab\chi & \chi(3b^2 - T_2) \end{pmatrix}. \quad (39)$$

Since  $T_1 = T_2$  we get for RPA frequencies

$$\Omega_i = \sqrt{\frac{4}{3} \left[ (T_1 \chi)^2 - 3 \pm \sqrt{9 + 3(T_1 \chi)^2} \right]}, \quad i = 1, 2. \quad (40)$$

In the limit of zero temperature,  $T_3 \rightarrow 0$ ,  $T_i \rightarrow 1$ ,  $i = 1, 2$ , the RPA frequencies reduce to the ones given in ref.[6],

$$i = 1, 2 \quad \Omega_i = \begin{cases} \sqrt{1 - \chi^2}, \sqrt{4 - \chi^2}, & |\chi| < 1 \\ \sqrt{2(\chi^2 - 1)}, \frac{1}{2} \sqrt{3(\chi + 3)(1 - \chi)}, & 1 < |\chi| < 3 \\ \sqrt{\frac{4}{3} [\chi^2 - 3 \pm \sqrt{3\chi^2 + 9}]}, 0, & |\chi| > 3 \end{cases}$$

In Fig. 2 (a) and (b) the RPA frequencies are represented respectively for  $\chi = -2$  and  $\chi = -6$ .

We conclude that the parameter which defines the behavior of the system is  $\chi' = T_1 \chi$ .

We notice that for finite temperatures the third mode is excited whereas it remains inert for zero temperature and also for the strong coupling regime. This feature of temperature dependence of small frequency modes is also described in ref. [8].

## IV. LARGE AMPLITUDE MOTION IN THE STRONG COUPLING

### REGIME

We turn now to the discussion of large amplitude motion. In what follows we restrict ourselves to the SCR where we are able to find canonically conjugate variables and study the stationary points in complete analogy to ref. [1]. For the strong coupling regime just mentioned we have two canonical variable pairs defined as follows\*

$$\gamma_1 = z_1 \frac{\sin \sqrt{z_1 z_1^*}}{\sqrt{z_1 z_1^*}} \cos \sqrt{z_2 z_2^*} \tilde{T}, \quad (41)$$

$$\gamma_2 = z_2 \frac{\sin \sqrt{z_2 z_2^*}}{\sqrt{z_2 z_2^*}} \sqrt{\tilde{T}}, \quad (\tilde{T}_1 = \tilde{T}_2 = \tilde{T}). \quad (42)$$

In terms of these variables eq.(14) reduces to

$$\text{Tr}(DU\dot{U}^\dagger) = \frac{1}{2} \sum_{i=1}^2 \dot{\gamma}_i \gamma_i^* - \gamma_i \dot{\gamma}_i^*. \quad (43)$$

The classical Hamiltonian is given by

$$\begin{aligned} \mathcal{H}_{cl} = & -\tilde{T} + 2\gamma_2 \gamma_2^* + \gamma_1 \gamma_1^* + \frac{V}{2} \left\{ -(\tilde{T} - \gamma_1 \gamma_1^* - \gamma_2 \gamma_2^*) \right. \\ & \left. (\gamma_1^2 + \gamma_1^{*2} + \gamma_2^2 + \gamma_2^{*2}) + (\gamma_1^* \gamma_2)^2 + (\gamma_1 \gamma_2^*)^2 \right\}. \end{aligned} \quad (44)$$

One of the temperature effects on this dynamics is to restrict the phase space of the system (see eq.(41) and (42))

\* Note that in this work "T" does not stand for temperature.

$$0 \leq \gamma_2 \gamma_2^* \leq \tilde{T} \quad (45)$$

and

$$0 \leq \frac{\gamma_1 \gamma_1^*}{\tilde{T} - \gamma_2 \gamma_2^*} \leq 1. \quad (46)$$

We found it is convenient to express the classical Hamiltonian in terms of the new variables

$$\gamma_2 = \sqrt{I_2} e^{i\theta_2}, \quad \gamma_1 = \sqrt{I_1} e^{i\theta_1}, \quad (47)$$

with the range of allowed values

$$0 \leq I_1 + I_2 \leq \tilde{T}. \quad (48)$$

In the large  $N$  limit (classical limit) the classical scaled Hamiltonian is defined as

$$\begin{aligned} E = \frac{\mathcal{H}_{cl}}{N} = & -T + 2\eta_2 + \eta_1 + \chi \left\{ -(T - \eta_1 - \eta_2) [\eta_1 \cos(2\theta_1) + \eta_2 \cos(2\theta_2)] + \right. \\ & \left. + \eta_1 \eta_2 \cos[2(\theta_1 - \theta_2)] \right\} \end{aligned} \quad (49)$$

with

$$\eta_1 = I_1/N, \quad \eta_2 = I_2/N, \quad T = \tilde{T}/N \quad \text{and} \quad 0 \leq \eta_1 + \eta_2 \leq T.$$

In the limit of zero temperature we recover the result previously obtained in ref.[1], (see eq. (2.9)).



In the  $SU(2)$  limit, i.e.,  $\eta_2 = 0$  we recover the finite temperature  $SU(2)$  result [9].

## V. FIXED POINTS AND BIFURCATIONS IN THE STRONG COUPLING REGIME

The equations of motion for the strong coupling regime are given by

$$\dot{\eta}_1 = -\frac{\partial E}{\partial \theta_1} = 2\eta_1\chi \{-(T - \eta_1 - \eta_2) \sin(2\theta_1) + \eta_2 \sin[2(\theta_1 - \theta_2)]\}, \quad (50)$$

$$\dot{\eta}_2 = -\frac{\partial E}{\partial \theta_2} = -2\eta_2\chi \{(T - \eta_1 - \eta_2) \sin(2\theta_2) + \eta_1 \sin[2(\theta_1 - \theta_2)]\}, \quad (51)$$

$$\dot{\theta}_1 = \frac{\partial E}{\partial \eta_1} = 1 + \chi \{-(T - 2\eta_1 - \eta_2) \cos(2\theta_1) + \eta_2 [\cos(2\theta_2) + \cos[2(\theta_1 - \theta_2)]]\}, \quad (52)$$

$$\dot{\theta}_2 = \frac{\partial E}{\partial \eta_2} = 2 + \chi \{\eta_1 [\cos(2\theta_1) + \cos[2(\theta_1 - \theta_2)]] - (T - \eta_1 - 2\eta_2) \cos(2\theta_2)\}. \quad (53)$$

The variables  $\eta_1$  and  $\eta_2$  are directly connected to the population of the levels. The model has a very rich classical structure which has been previously studied in the zero temperature limit [1]. We have studied the stationary points analytically. In

Table I we give the energies, coordinates and validity range of the solutions at finite temperature. In Fig. 3 we display the zero temperature results for attractive and repulsive interactions. It is important to notice the difference on the bifurcations of minima in the two cases. For negative  $\chi$  values we have two bifurcations of equilibrium: we find four minima ( $N$  solution) for  $\chi \leq -3$  which bifurcate to two minima at  $\chi = -3$  and stay that way in the interval  $-3 \leq \chi \leq -1$  ( $K$  solution) and bifurcate again to one single minimum for  $\chi \leq -1$  ( $H$  solution). The positive  $\chi$  values present two minima for  $\chi \geq 1$  ( $A$  solution) and only one bifurcation to one minimum for  $\chi \leq 1$  ( $H$  solution).

In Figs. 4(a) and (b) we show the behavior of the energy of the fixed points as a function of  $\chi$  (zero temperature) and  $T(\beta)$  ( $\chi = -6$ ) respectively. Here we observe that the main temperature effect in the SCR is to “weaken” the coupling, i.e., increasing the temperature in Fig. 4(b) corresponds to decreasing  $\chi$  in Fig. 4(a), qualitatively speaking. In fact there is no scaling behavior as can be clearly seen in Table I. We have not undertaken this study for the other two regimes but we expect that the temperature effects there will be more dramatic (see eq. (19)).

## VI. POINCARÉ SECTIONS OF THE THERMAL DYNAMICS IN THE SCR

The Poincaré sections as a function of temperature show that although there is no

scaling, near the minimum solution the temperature qualitatively does not change the behavior of the system. Note that because of the shrinking effect, it is complicated to compare sections of different temperatures in order to look for new effects brought by the temperature. In Fig. 5 (a), (b), (c) and (d) we show the Poincaré sections for zero temperature  $\chi = -6$  near the equilibrium point  $N$ . They should be compared to Fig. 6 (a), (b), (c) and (d) where the same is calculated for finite temperature. We have also studied the Poincaré sections at the bifurcation point (when the  $N$  solution merges into the  $K$  solution) for  $\chi = 6.0$  at phase transition inverse temperature  $\beta_{cr1}$  (Fig. 7) and for  $\chi = 3.0$  at zero temperature (Fig. 8).

## VII. CONCLUSION

In the present work we have studied the  $SU(3)$  Lipkin Model within a thermal mean field approach. We have explicitly shown that one remarkable effect of the temperature is giving rise to a new degree of freedom “frozen” in the zero temperature limit.

The dynamical equations of motion exhibit a very rich structure. Temperature brings in new nonlinear terms, thus altering the structure of the equation in a more radical way than has been found in the Maser Model [4]. Although we have not been able to find three pairs of canonically conjugate variables for the most general situation, we have shown that the strong coupling situation can be described by

two pairs of such variables. In this case we have discussed the dynamics in detail: the behavior of fixed points and bifurcations as well as their existence conditions as function of temperature and coupling strength are studied.

We find that net effect of temperature is to “weaken” the coupling strength, but this relation is highly non trivial. Although the new terms in the Hamiltonian show a rather nonlinear behavior with temperature (e.g. it does not consist of pure scaling effect), in the SCR this is not observed in the Poincaré sections.

## ACKNOWLEDGEMENTS

We gratefully acknowledge many groups discussions with the colleagues K. Furuya, F. Camargo, G. Pellegrino (UNICAMP), A.F.R. de Toledo Piza and M. Trindade dos Santos (USP). We would like to thank C.H. Lewenkopf (Un. of Washington) for the Poincaré sections programme. This work was partially supported by JNICT, CNPq and FAPESP.

## Referências

- [1] P.Lebouf and M.Saraceno, Phys.Rev. A **41**, 4614 (1990).
- [2] D.C.Meredith, S.E.Koonin and M.R.Zirnbauer, Phys.Rev. A **37**, 3499 (1988).
- [3] J.da Providência and C.Fiolhais, Nucl.Phys. A **435**, 190 (1985); M.Yamamura, J.da Providência and A.Kuriyama, Nucl.Phys. A **514**, 461 (1990); M.Yamamura, J.da Providência, A.Kuriyama and C.Fiolhais, Prog.Theor.Phys. **81**, 1198 (1989).
- [4] A.H.Blin, B.Hiller, M.C.Nemes e J.Providencia, J.Phys. A **25**, 2243 (1992).
- [5] S.Y.Li, A.Klein and R.M.Dreizler, J.Math.Phys. **11**, 975 (1970); E.Moya de Guerra and F.Villars, Nucl.Phys. A **298**, 109 (1978); P.Lebouf and M.Saraceno, J.Phys. A **23**, 1745 (1990); P.Lebouf, D.C.Meredith and M.Saraceno, Ann.Phys.(NY) **208**, 333 (1991).
- [6] R.D.Williams and S.E.Koonin, Nucl.Phys. A **391**, 72 (1982).
- [7] M.O.Terra, A.H.Blin, B.Hiller, M.C.Nemes, C.Providência and J. da Providência, “*The SU(3) Lipkin model: (I) The thermodynamics.*”, to be published.
- [8] J.da Providência, M.Yamamura and A.Kuriyama, Phys.Rev. C **50**, 1720 (1994).
- [9] M.O.Terra, A.H.Blin, B.Hiller, M.C.Nemes, C.Providência and J. da Providência, J.Phys. A **27**, 697 (1994).

## FIGURE CAPTIONS

FIG. 1. Plot of  $T_1$ ,  $T_2$  and  $T_3$  as function of the inverse temperature  $\beta$  of the system for  $\chi = -6.0$ . The values of the critical inverse temperatures  $\beta_{cr1}$  and  $\beta_{cr2}$  at which there are phase transitions are shown and the three phases (strong (SCR), intermediate (ICR) and weak (WCR) coupling regimes) are separated by a vertical dotted line. Note that in the SCR,  $T_3$  vanishes and  $T_1$  and  $T_2$  have the same value.

FIG. 2. RPA frequencies as function of the inverse temperature  $\beta$  of the system for (a)  $\chi = -2.0$  and (b)  $\chi = -6.0$ . Note the “awakening” of the third mode in the  $SCR \rightarrow ICR$  phase transition.

FIG. 3. Classical energy of stationary points as function of coupling parameter  $\chi$  at zero temperature. These points are labeled from  $A$  to  $N$ . The point  $G$  can be found numerically and it is of few importance here. For attractive interaction there are three minimum solutions ( $N$  (four minima),  $K$  (two minima) and  $H$  (one minimum)). For repulsive interaction there are just two minimum solutions ( $A$  (two minima) and  $H$  (one minimum)). The ground state energy phase transitions are related with the thermodynamical phase transitions.

FIG. 4. Classical energy of stationary points as function of (a)  $\chi$  for zero temperature and (b)  $T(\beta)$  for  $\chi = -6.0$  in the SCR. Note the disappearance of the solutions with temperature increase as well as with  $|\chi|$  decrease.

FIG. 5. Poincaré sections for several trajectories at zero temperature and  $\chi = -6.0$

near the minimum point (solution  $N$ ) through the plane  $\eta_2 = 0.166$  for (a)  $E = -2.1$ , (b)  $E = -2.07$ , (c)  $E = -2.05$  and (d)  $E = -2.03$ . They are displayed in polar variables  $(\eta_1, \theta_1)$  for the upper hemisphere ( $0 \leq \theta_1 \leq \pi$ ).

FIG. 6. Poincaré sections for several trajectories at finite temperature  $\beta = 0.62$  ( $T(\beta) = 0.902$ ) and  $\chi = -6.0$  near the minimum point through the plane  $\eta_2 = 0.1340$  for (a)  $E = -1.75$ , (b)  $E = -1.73$ , (c)  $E = -1.72$  and (d)  $E = -1.70$ .

FIG. 7. Poincaré sections for several trajectories at the  $SCR \rightarrow ICR$  phase transition temperature ( $T(\beta) = 0.5$ ) and  $\chi = -6.0$ . The sections were made through the plane  $\eta_2 = 0.05$  for  $E = -0.47$ .

FIG. 8. Poincaré sections for several trajectories at zero temperature and  $\chi = -3.0$  near the points  $K$  and  $N$ . The sections were made through the plane  $\eta_2 = 0.05$  for  $E = -1.2$ .

### TABLE CAPTIONS

TABLE I. Energy, coordinates  $(\eta_1, \eta_2, \theta_1, \theta_2)$  and range of validity as function of coupling parameter  $\chi$  and temperature of thirteen of the fourteen fixed points of classical Hamiltonian (49) for strong coupling regime ( $T_1 = T_2 = T$ ). These points are labeled from  $A$  to  $N$ . The point  $G$  can be found numerically and it is of few importance here.

Figure 1

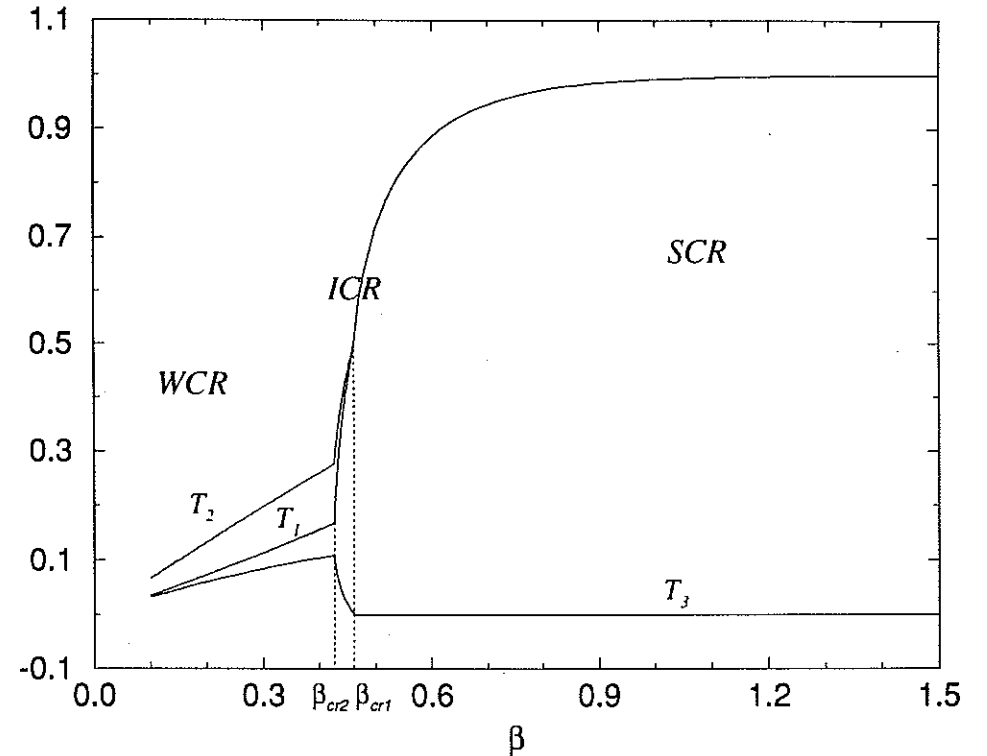


Figure 2(a)

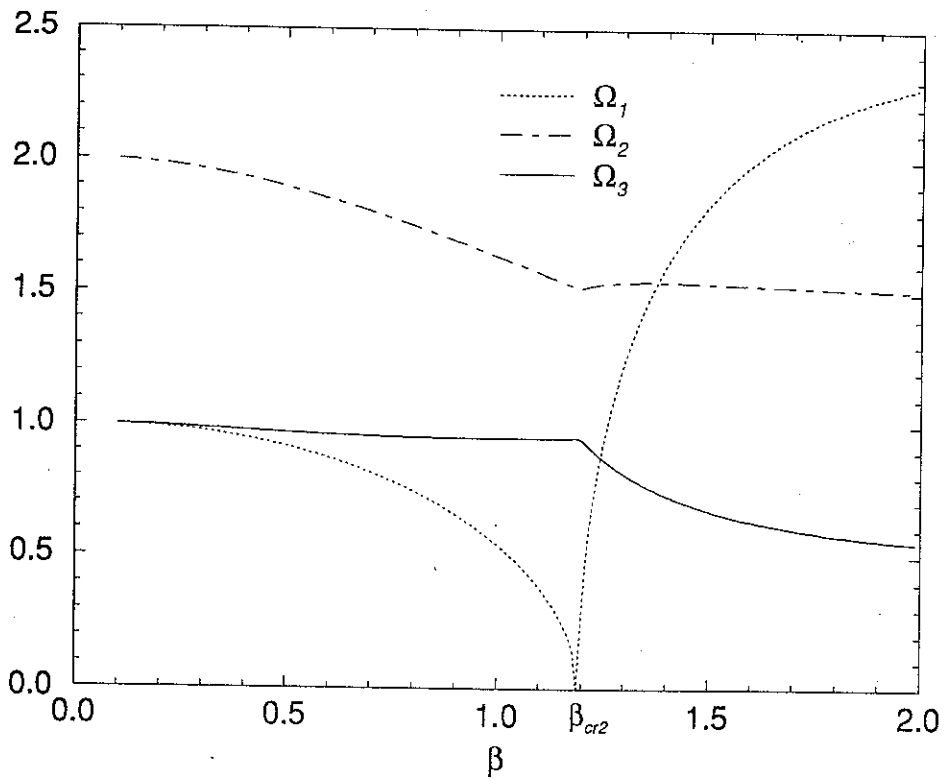
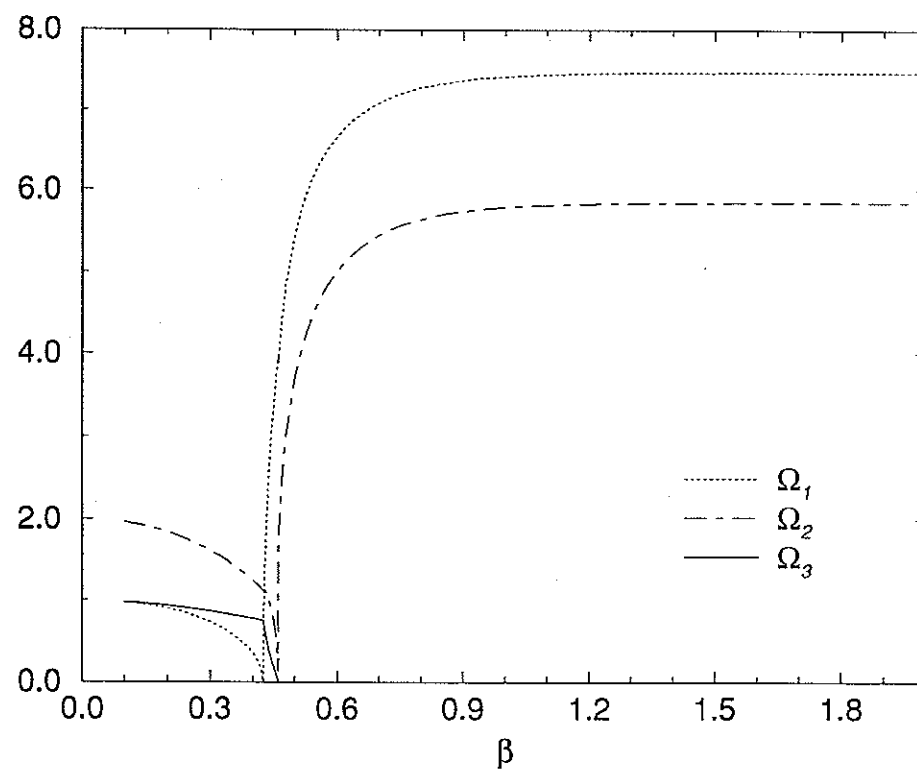


Figure 2(b)



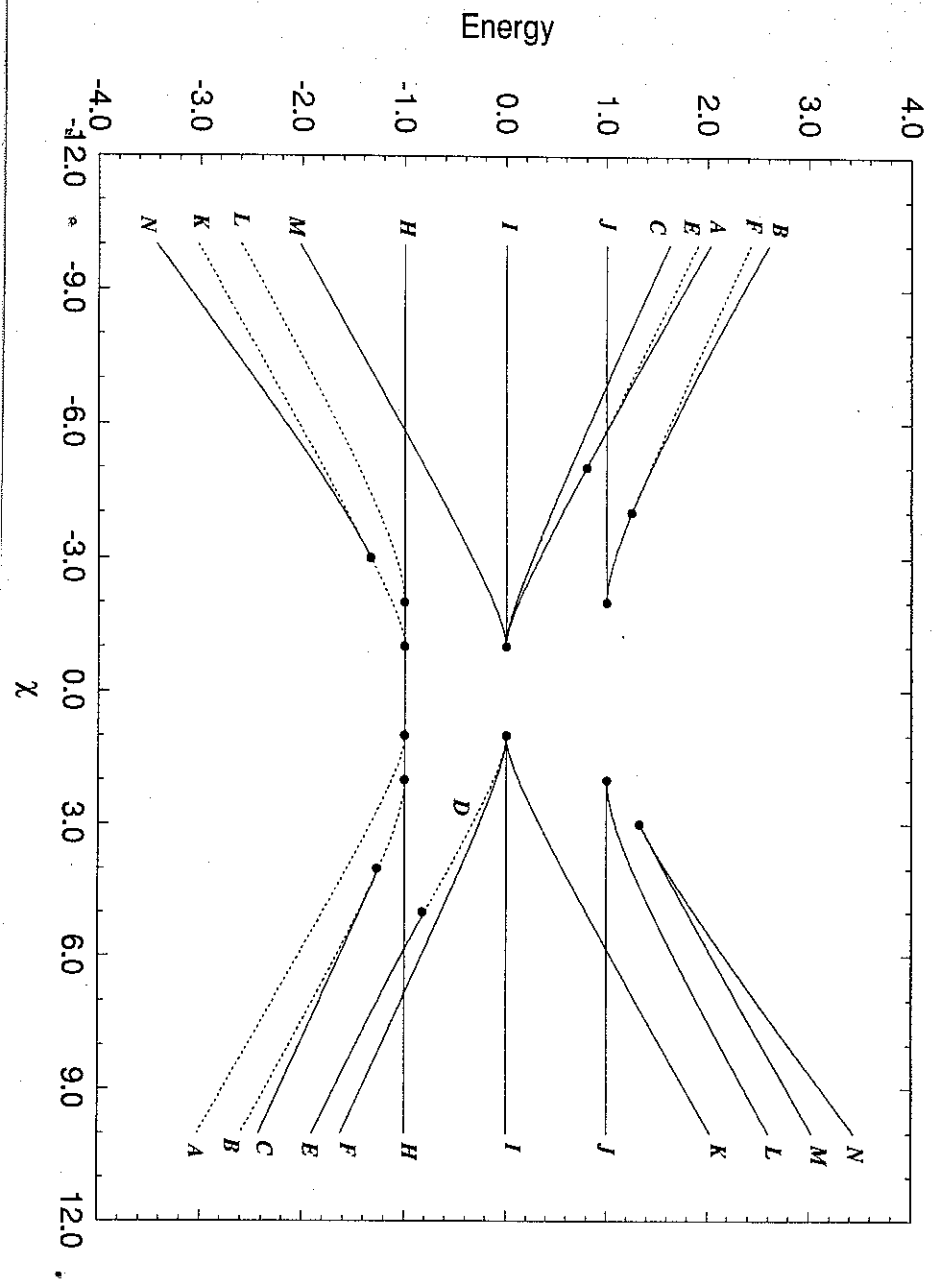


Figure 3

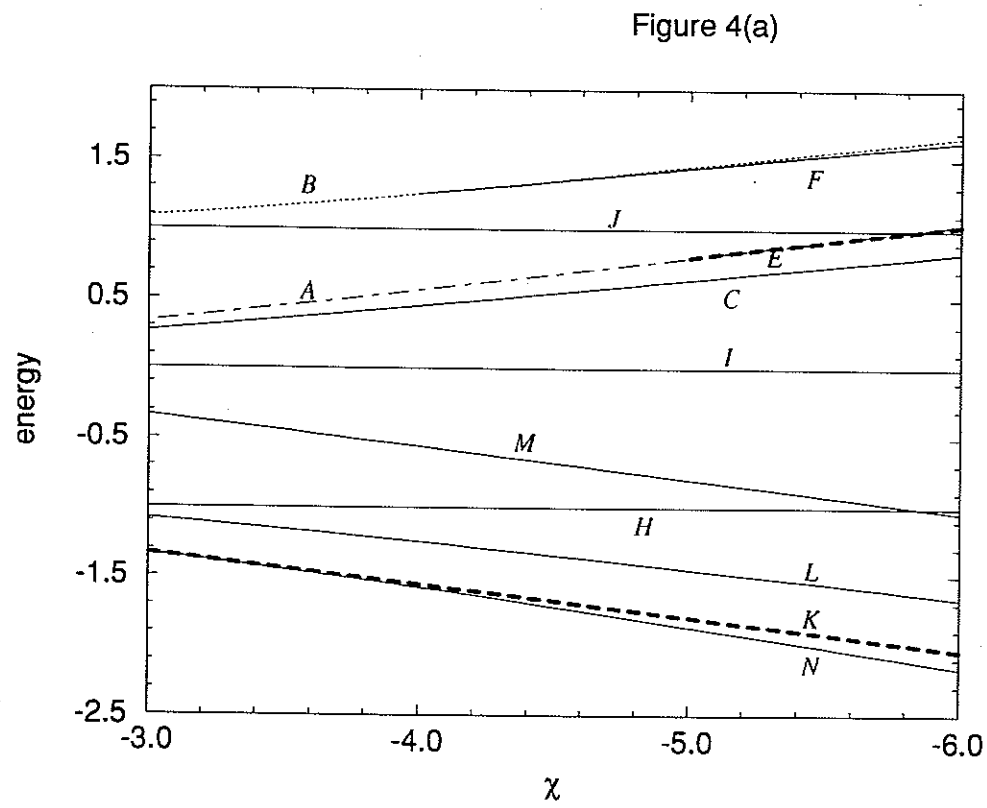


Figure 4(a)

Figure 4(b)

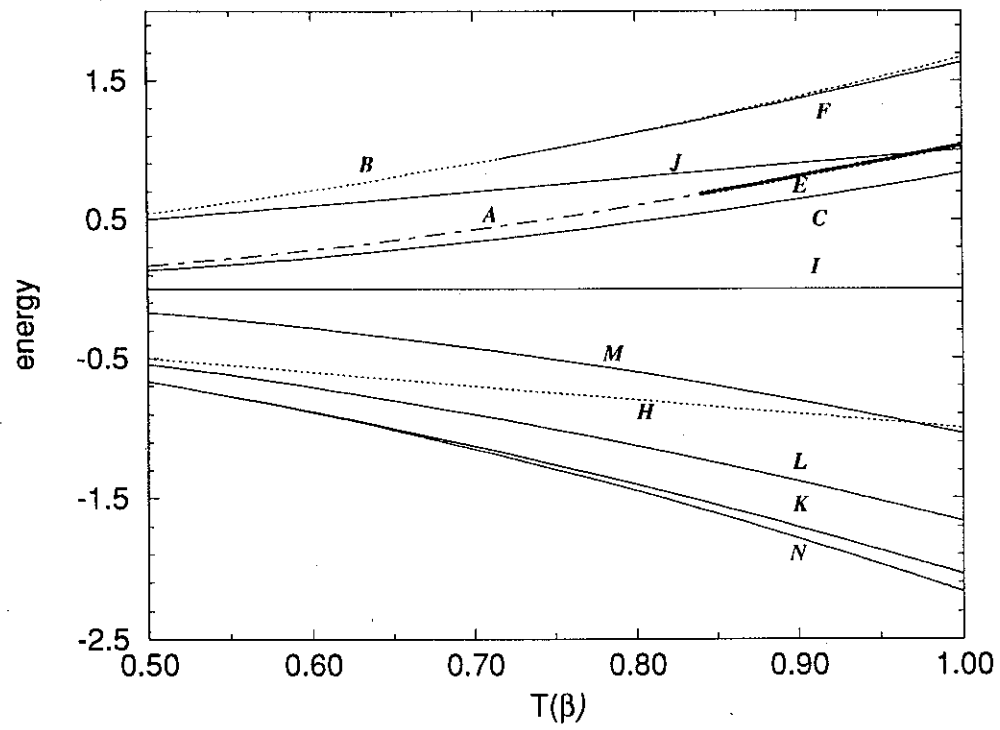


Figure 5(a)

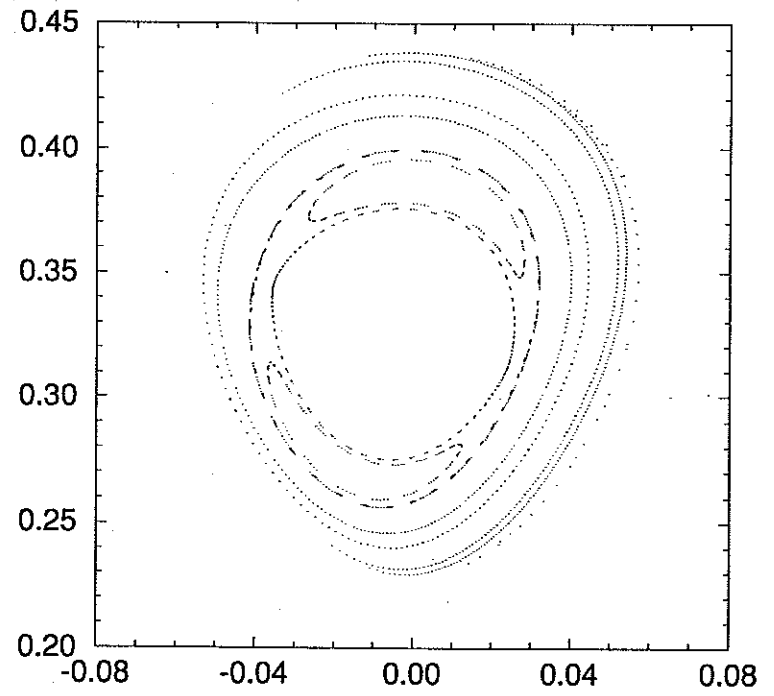


Figure 5(b)

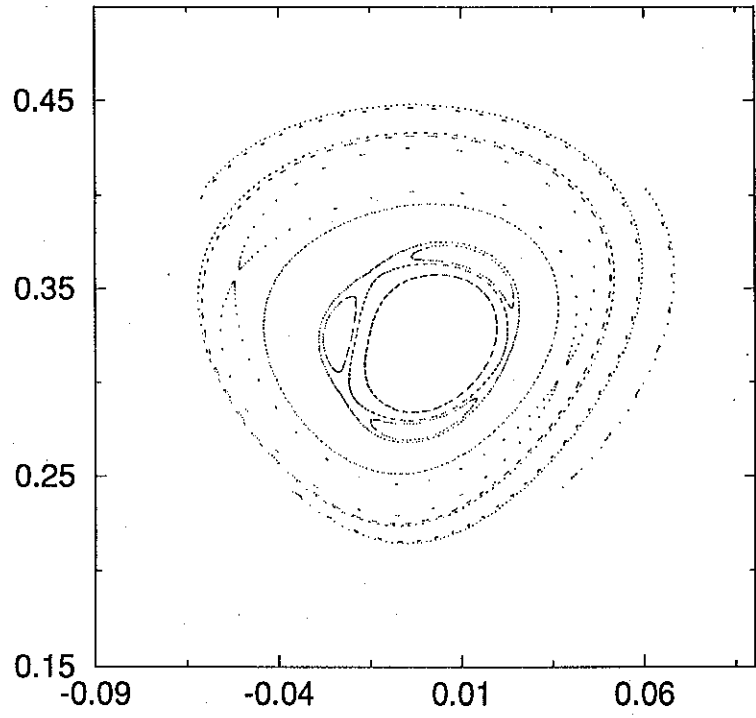


Figure 5(c)

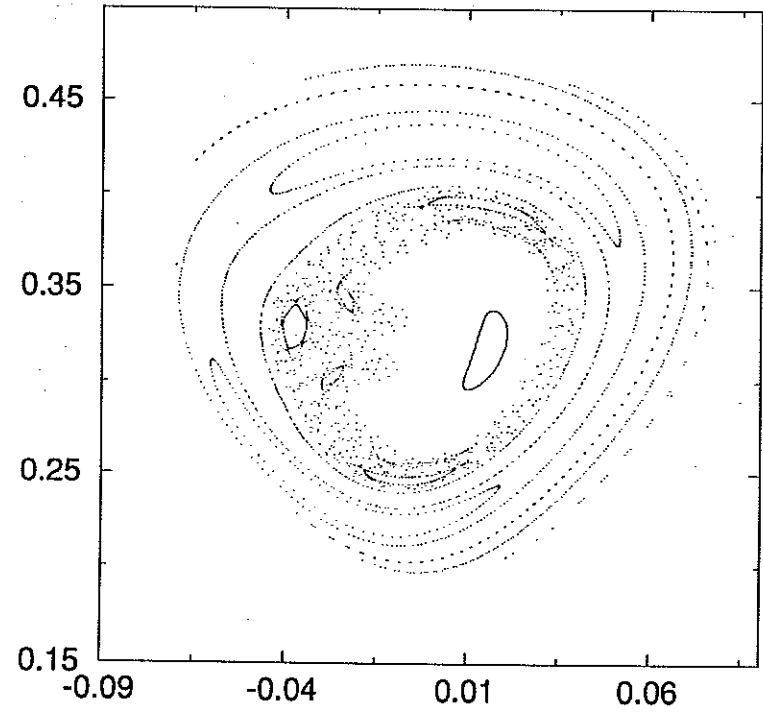




Figure 5(d)

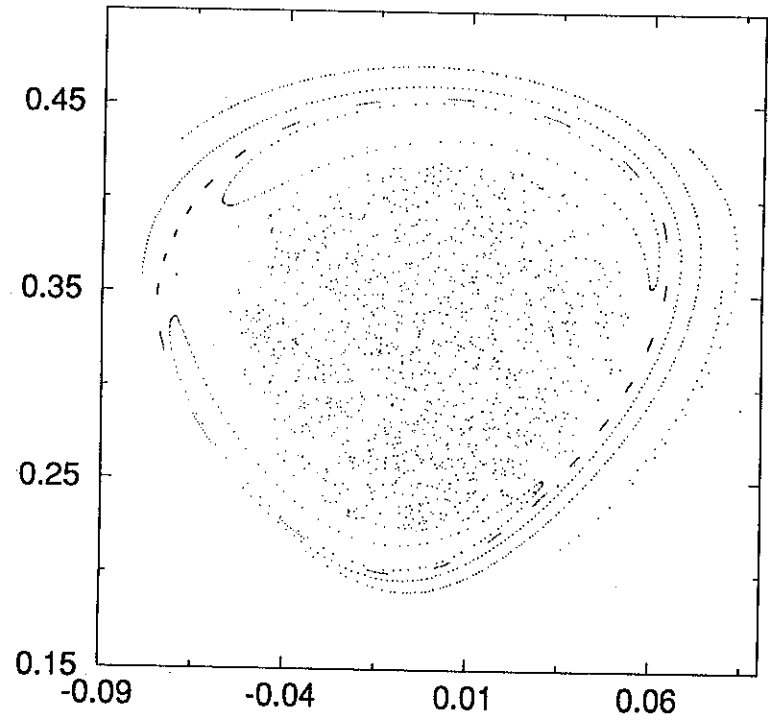


Figure 6(a)

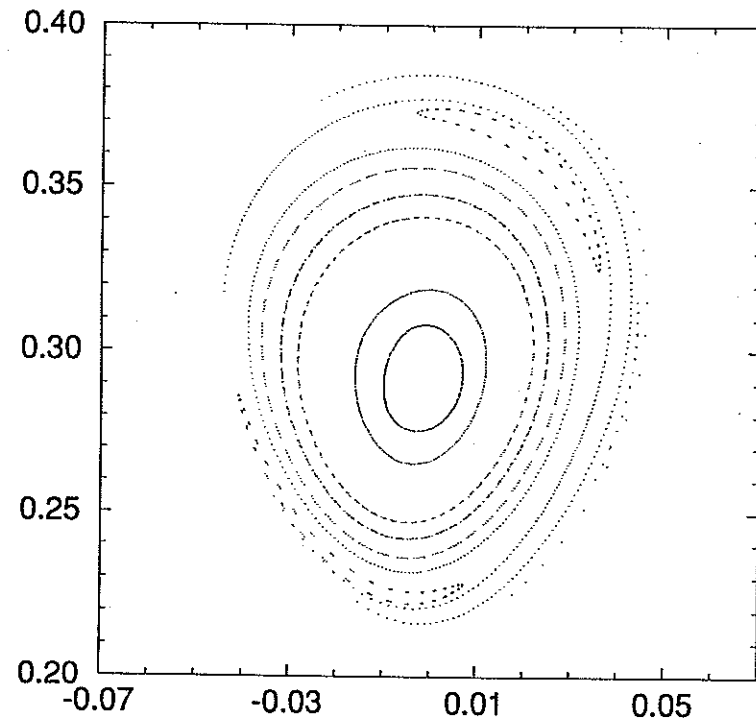


Figure 6(b)

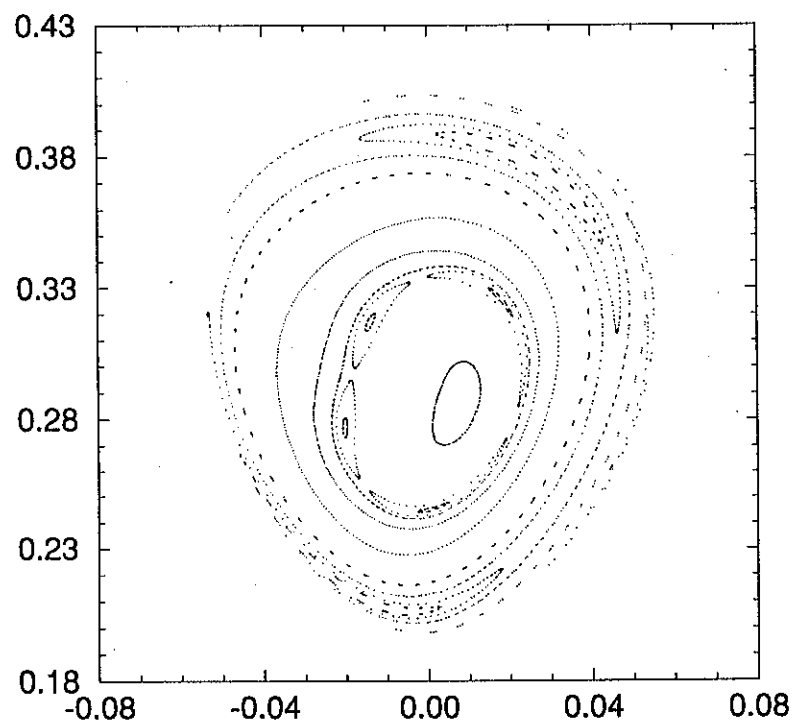


Figure 6(c)

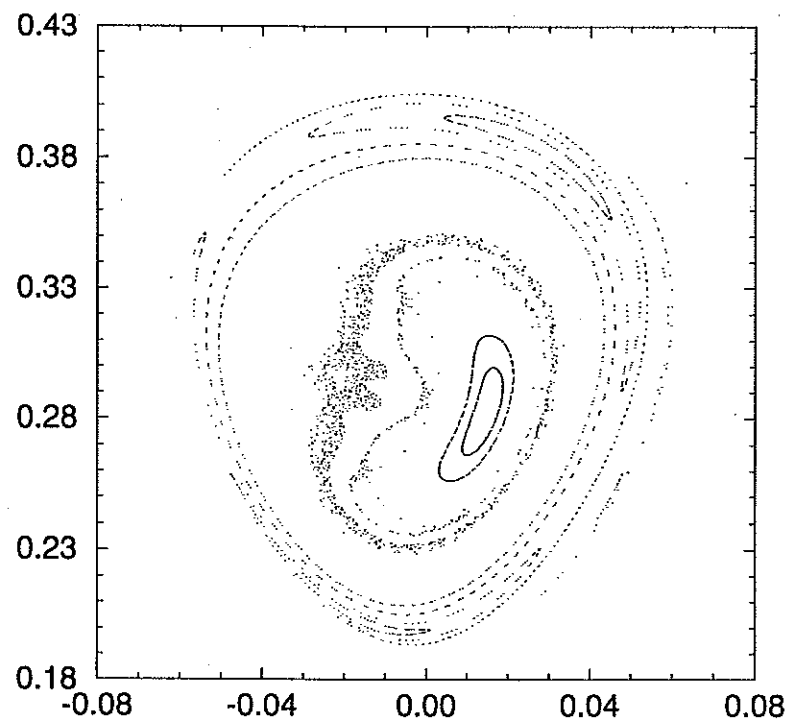


Figure 6(d)

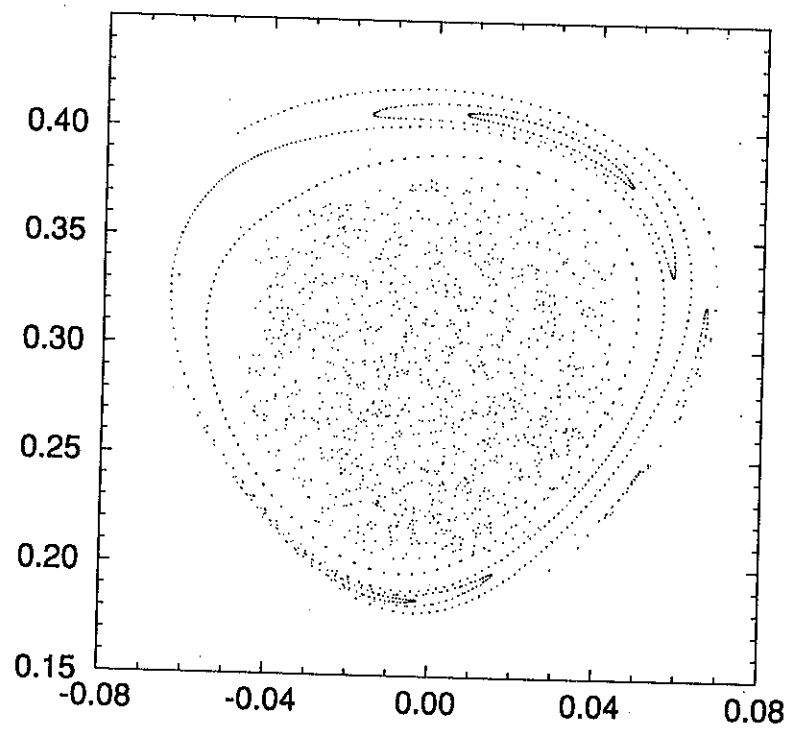


Figure 7

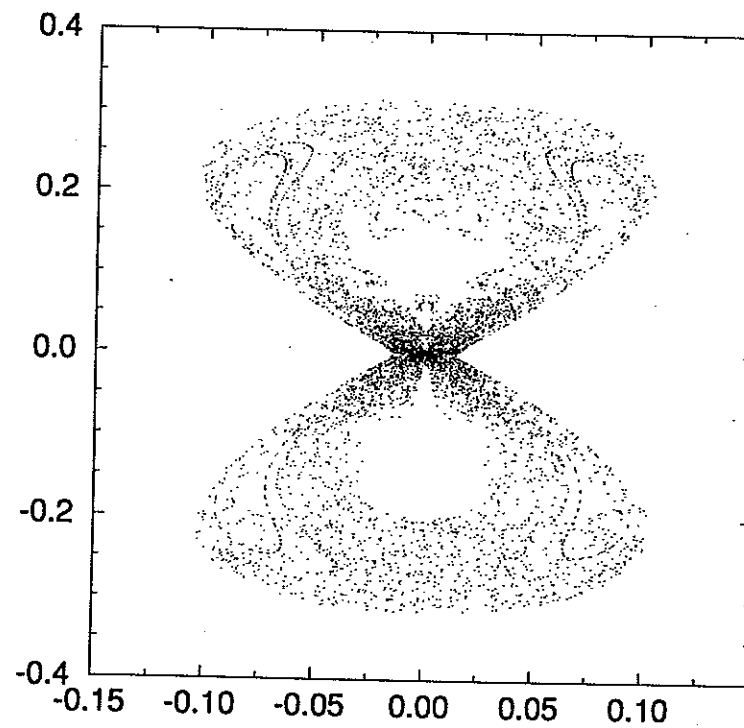
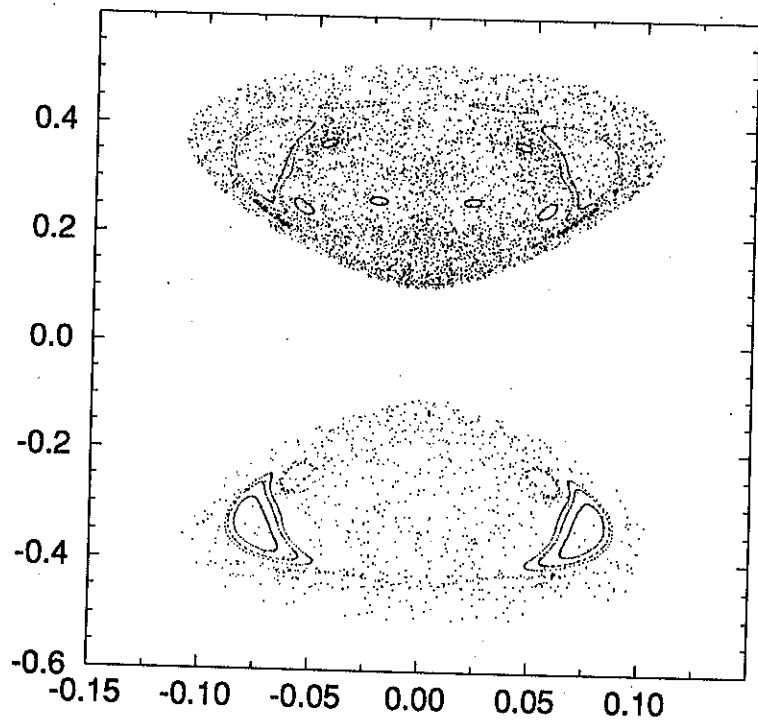


Figure 8



Point	$E$	$\eta_1$	$\eta_2$	$\theta_1$	$\theta_2$	Validity
A	$-\frac{(\chi T+1)^2}{4\chi}$	$\frac{\sqrt{T}-1}{2\chi}$	0	0	-	$ \chi T  \geq 1$
B	$-\frac{(\chi^2 T^2+4)}{4\chi}$	0	$\frac{\sqrt{T}-2}{2\chi}$	-	0	$ \chi T  \geq 2$
C	$-\frac{(\sqrt{T+1})^2}{5\chi}$	$\frac{\sqrt{T}-4}{5\chi}$	$\frac{\sqrt{T}+1}{5\chi}$	0	0	$\chi T \leq -1$ or $\chi T \geq$
D	$-\frac{(\sqrt{T-1})^2}{4\chi}$	$\frac{\sqrt{T}+1}{2\chi}$	$\frac{\sqrt{T}-1}{2\chi}$	$\theta_2 + \frac{\pi}{2}$	$\cos(2\theta_2) = \frac{3-\sqrt{T}}{2}$	$1 \leq \chi T \leq 5$
E	$-\frac{(\chi^2 T^2-5)}{5\chi}$	$\frac{3T}{5}$	$\frac{\sqrt{T}+5}{5\chi}$	0	$\frac{\pi}{2}$	$ \chi T  \geq 5$
F	$-\frac{(\sqrt{T-1})^2}{5\chi}$	$\frac{\sqrt{T}+4}{5\chi}$	$\frac{3(\sqrt{T}-1)}{5\chi}$	$\frac{\pi}{2}$	0	$\chi T \leq -4$ or $\chi T \geq$
H	$-T$	0	0	-	-	$\forall \chi, T$
I	0	$T$	0	$\cos(2\theta_1) = \frac{-1}{\sqrt{T}}$	-	$ \chi T  \geq 1$
J	$+T$	0	$T$	-	$\cos(2\theta_2) = \frac{-2}{\sqrt{T}}$	$ \chi T  \geq 2$
K	$\frac{(\sqrt{T-1})^2}{4\chi}$	$\frac{\sqrt{T}+1}{2\chi}$	0	$\frac{\pi}{2}$	-	$ \chi T  \geq 1$
L	$\frac{\sqrt{2T^2+4}}{4\chi}$	0	$\frac{\sqrt{T}+2}{2\chi}$	-	$\frac{\pi}{2}$	$ \chi T  \geq 2$
M	$\frac{(\sqrt{T+1})^2}{4\chi}$	$\frac{\sqrt{T}-1}{2\chi}$	$\frac{\sqrt{T}+1}{2\chi}$	$\cos(2\theta_1) = \frac{-(\sqrt{T}+3)}{2\sqrt{T}}$	$\theta_1$	$\chi T \leq -1$ or $\chi T \geq$
N	$\frac{\sqrt{2T^2+3}}{3\chi}$	$\frac{T}{3}$	$\frac{\sqrt{T}+3}{3\chi}$	$\frac{\pi}{2}$	$\frac{\pi}{2}$	$ \chi T  \geq 3$

Table I